An Analytical Framework for Evaluating the Impact of Distribution-Level LVRT Response on Transmission System Security

An Analytical Framework for Evaluating the Impact of Distribution-Level LVRT Response on Transmission System Security

Pouya Salyani, Kazem Zare, Mehdi Abapour, Amin Safari and Miadreza Shafie-khah, *Senior Member, IEEE*

***Abstract*—Low voltage ride through (LVRT) is a solution to increase the tolerance of distributed energy resources (DERs) against the voltage sags. However, the possibility of DERs trip according to the present grid codes exists. Such trips do not have a substantial local effect but are essential for transmission systems with connected DER-penetrated distribution networks (DPDNs). This paper investigates an analytical framework to see the impact of distribution-level LVRT response on transmission system security. LVRT response stands for the total amount of lost DER capacity due to the inability to meet the LVRT requirement during the voltage sag. This generation loss in the distribution sector can expose the transmission network to lines overloading after fault clearance. The proposed novel approach is based on a source contingency analysis that lets transmission system operators (TSOs) conduct an LVRT-oriented security assessment. In this kind of security assessment, a mathematical function is defined as the LVRT response function of DPDNs. This function gives the lost DER capacity in response to the transmission-level transient faults and is constructed by distribution system operators (DSOs). The TSO can use these functions to assess the loading security of transmission lines in post-clearance system conditions. In this analytical framework, LVRT-oriented security is evaluated by calculating the risk of lines overloading under a large number of random faults. The proposed approach is implemented in two test power systems with a considerable DER penetration level to obtain the risk of line overloading due to the LVRT response in distribution networks.**

***Index Terms*—LVRT, DER, voltage sag, transmission system security, Haar expansion.**

NOMENCLATURE

Sets

Ω_B	Set of buses
Ω_L	Set of transmission lines
Ω_T	Set of fault types

Superscripts

$*$	Reference
$\pm$	Positive and negative sequences
fc	Fault clearing time
fl	Faulted line
ft	Fault type
pc	Pre-contingency
sg, ig	Synchronous and inverter-interfaced generators

Parameters

$\bar{\tau}, \underline{\tau}$	Upper and lower bounds of sag duration
$\bar{\zeta}, \underline{\zeta}$	Upper and lower bounds of sag depth
$\bar{J}_\ell$	Line flow limit
γ_i	1 if a DPDN is connected to bus i
λ	Fault rate
A	Incidence matrix of transmission system
G, B	Conductance and susceptance
N_s	Number of MCS iterations
p	Probability
P_i^d, Q_i^d	pre-fault active and reactive load connected to bus i
P_i^g, Q_i^g	pre-fault active and reactive power of generator connected to bus i
S_b	Base power

Variables and functions

χ	Binary Variable that is 1 if any line is overloaded
δ	Frame angle in radian
Γ	Risk of security violation for transmission system
$\mathbf{\Lambda}, \mathbf{U}$	Coefficient and output matrices
$\Re(.)$	Random number generation function
τ	Sag duration
$\mathbf{x}, \mathbf{z}, \mathbf{u}$	Differential, algebraic and input vectors
θ	Bus angle in radian
$\varphi(.)$	Scaling function

ζ	Sag depth
$F(.)$	Probability distribution function
$H(.)$	Haar series function
J	power flow in transmission line
K	Haar series coefficient
P_i^{sr}	spinning reserve of generator connected to bus i
V, I	Voltage, current

Acronyms

DAE	Differential-Algebraic Equations
DER	Distributed Energy Resources
DPDN	DER-penetrated Distribution Networks
DSO	Distribution System Operator
LVRT	Low Voltage Ride Through
MCS	Monte Carlo Simulation
PCC	Point of Common Coupling
T&D	Transmission and Distribution
TSO	Transmission System Operator

I. Introduction

USAGE of DERs in power systems has been considerably grown in the recent decade. Despite the undeniable advantages of DERs in various aspects of power systems, their high penetration in distribution networks entails a significant problem. In the past standards, the DERs had to be tripped by any voltage drop in their PCC. This issue had a main drawback: the sudden loss of a high generation amount in the distribution sector. This sudden generation loss is dangerous for the power system and may lead to cascading outages and blackouts.

LVRT was introduced as a new grid code, which states that the DERs can stay connected during the voltage sag via reactive current injection [1] and according to the mandated standards. In 2018, the IEEE 1547 standard defined three categories of operating performance in voltage abnormal conditions for DERs [2]. The abnormal voltage condition consists of both overvoltage and undervoltage in the distribution network. Category I performance provides the minimal reliability requirements of bulk power systems and is attainable by all existing DER technologies. Category II is developed to cover all bulk system reliability requirements and avoid adverse tripping of DERs during a wide range of disturbances. Category III performance is designed for all reliability requirements of bulk power systems with a high penetration level of DER and provides the highest LVRT capability.

Based on this standard, synchronous hydro and turbine-driven generators like Diesel engine generators (DEGs) and inverter-interfaced fuel cells have Category I performance. Inverter-interfaced photovoltaic (PV) and energy storage systems and all types of wind turbine generators are accounted as Category II DERs. Category III is specific for PV, and its application depends on technical issues, penetration level, and the operator's decision. Fig. 1 depicts Category II LVRT performance, which specifies five regions at all. When the PCC voltage falls within region 3, the DER shall be tripped, but the performance in regions 1 and 2 permits to ride through the abnormal voltage condition. Regions 4 and 5 can take one of the ride-through, momentary cessation, or trip performances for the DER.

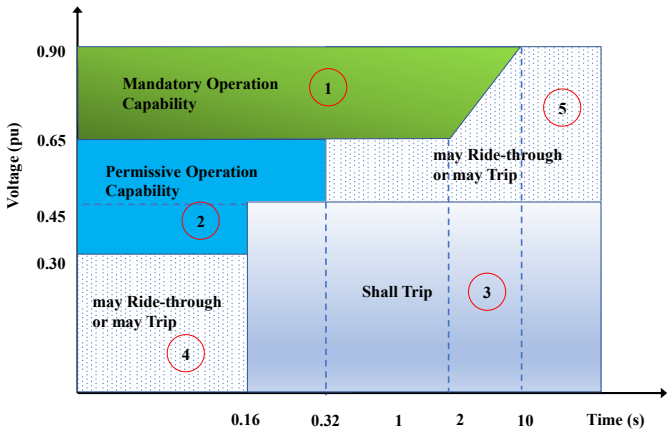

Fig. 1. Response of Category II DERs to voltage sags.

LVRT has been studied in limited contexts, and LVRT improvement of inverter-interfaced DERs with different control methods has been one of the main concerns [3]–[8]. These control strategies are defined for both the balanced and unbalanced voltage sag conditions [9]. Transient stability analysis concerning the LVRT feature of the DERs is another issue that has been considered in past years [10]–[13]. Furthermore, a significant problem is the fault currents of inverter-interfaced DERs in the abnormal voltage condition and during the LVRT performance. Authors in [14] investigated an LVRT-based study of the fault currents within a probabilistic framework. Also, superconducting fault current limiters were proposed in [15] and [16] to deal with this problem.

Appropriate LVRT performance of a microgrid with multiple DERs implies a different control strategy. The neural network concept and consensus-based distributed control were carried out by [17] and [18] to improve the microgrid LVRT performance. The droop control method was applied by [19] and [20] to enhance the LVRT functionality of microgrids. A coordinated LVRT-based control strategy was proposed in [21] that takes into account the unbalanced voltage conditions. In addition, [22] and [23] addressed the control methods to enhance the LVRT of microgrids with weak grid connections.

The optimal design of active distribution networks, PV unit penetration level, and their converter size to enhance the LVRT capability were investigated in [24]. Ref. [25] studied the impact of PV penetration level on LVRT performance of distribution networks and improvement of the voltage instabilities. Moreover, [26] discussed the Fault Induced Delayed Voltage Recovery issue in distribution networks with different penetration levels of DERs and induction motors.

Here, an important point exists that has not been addressed in previous works yet. When a fault occurs in the transmission sector, a voltage sag appears in power system nodes with different depths and may affect a large area in the distribution sector. Notwithstanding the LVRT ability, the DERs' response differs, depending on the appeared voltage sag on their PCC and the sag duration. Therefore, it is possible for a part of these DERs to be tripped due to the incapability to meet the LVRT requirement. Furthermore, note that some DERs in the grid may not have the LVRT ability.

Ref. [27] gave a viewpoint about the LVRT performance of PVs in the distribution level and their impact on the whole power system. This study was carried out with simplifications and aggregation of PVs to reduce the problem complexity. Authors in [28] proposed a general mathematical model for DPDNs that determines the DERs with successful ride-through and the DERs that shall be tripped during the sag event. It gives the lost generation capacity of the DPDNs under various balanced voltage sags originating from the upstream grid. The value of lost DER capacity for a voltage sag with a certain depth and duration is defined as the LVRT response, varying from 0 to 100% of the installed capacity. 0 states the successful ride-through of all the DERs, and 100% stands for the failure of all DERs within the DPDN in meeting the LVRT requirement (resulting in their trip). This proposed model acts as a prerequisite for the new framework introduced herein.

This paper introduces a novel topic for the first time, the security assessment of transmission systems with the orientation of DPDNs' LVRT response. In fact, this security analysis relates to the post-clearance (after fault clearance) condition of the system and directly depends on the LVRT behavior of the DPDNs during the voltage sag. After fault clearance in the transmission sector, a part of DERs in the distribution sector may be tripped, resulting in the net load increase of the whole transmission system. This net load is the difference between the pure load of the DPDN and its DER generation capacity. Hence the net load increase is equivalent to the loss of DER generation. Besides the dynamic stability issues (ignored here), this net load increase can expose the transmission lines to overcurrent and cause their outage. When the system operates in the normal state, the TSO requires an analytical tool to assess the LVRT-oriented security as transient faults are probable in the system. To clarify, the essence of this work is the so-called source contingency, a branch of contingency analysis to assess the security of transmission systems with connected DPDNs. This source contingency indicated in [29] is based on the response of DERs to the voltage sags induced by the transmission-level faults. Using the source contingency, the LVRT-oriented security assessment can be conducted on the transmission system to evaluate the lines' loading security. In this analytical framework, the LVRT-oriented security assessment measures the risk of security violation with the help of MCS. The attained risk value is essential for the TSO to make appropriate decisions.

There exists an essential point. This is not a traditional security assessment problem, in which the line/generator contingency analysis is applied, and the system security is simply evaluated through the power flow. While in this work, the LVRT-oriented security assessment problem consists of two layers. The first layer is the LVRT analysis to find the tripped DER capacity in the faulty condition of the system. The second layer is the security assessment in the post-clearance condition of the system and finding the overloading risk for a large number of random faults. To solve this problem, one solution is the LVRT-based simulation of the T&D system to obtain the lost DER capacity for each fault and then calculate the overloading risk of the transmission system. The T&D simulation method has to meet the two mentioned layers, which definitely results in a high computational time. It is worth noting that the LVRT analysis majorly belongs to the distribution level, but the security assessment is conducted at the transmission level. On the other hand, a power system may include several numbers of DPDNs that are usually large-sized and raise the simulation time of the LVRT analysis. Furthermore, the DPDNs may involve different LVRT categories of DERs, which makes the simplification method questionable. Hence, it is not plausible for the TSO to implement the simulation method that

- involves both the T&D sectors and leads to a very complex modeling
- has to meet the two steps of LVRT analysis and security assessment

To this end, a mathematical function is defined for the LVRT response of the DPDNs. This function gets the sag depth and duration as the input and gives the lost DER capacity of the DPDN as the output. The function definition can be so helpful in this security assessment and resolves the need for LVRT analysis by the TSO. The DSOs construct these functions (as explained later) and then send them to the TSO. Thus, the TSO can use these functions to evaluate the system security in a short computation time, irrespective of modeling the distribution level. In more detail, the DSOs are responsible for constructing the LVRT response functions of the DPDNs through the LVRT analysis. These functions require an update by the DSO whenever a DPDN's DER capacity or network configuration is changed. Moreover, these functions are the LVRT capability characteristic of the DPDNs that can be implemented independently of the system's pre-contingency operating point. The pre-contingency operating point stands for the system secure condition before the source contingency analysis. The proposed framework helps the TSO carry out the source contingency analysis without any need for LVRT analysis (that must consider the distribution sector model).

To highlight the importance of this topic, a graphical explanation is provided in Fig. 2. This figure shows the modified six bus RBTS transmission system defined in Section III and includes three DPDNs. The figure illustrates the LVRT response impact on the transmission system loading security. The system is in the normal operation state, with a certain operating point. Fig. 2.a shows a transient three-phase (3PH) fault occurrence in line 2-4 of the transmission network with a duration of 400 ms. This fault as a disturbance causes a voltage drop in the grid and consequently entails the LVRT response of the DERs within the DPDNs to this abnormal voltage condition. Regarding the responses of DERs relative to the fault type, sag depth, and sag duration, the transmission

network faces an increase in the net load of the DPDNs after the fault clearance and in a dynamically stable condition of the network. The net load increase (loss of generation in the DPDNs) refers to the failure in meeting the ride-through requirement by some DERs. This is shown in Fig. 2.b, where the net loads of the three DPDNs connected to buses 3, 5, 6 are raised by 56, 11, and 16 MW, respectively. These values result from lost generation within the DPDNs, since a part of DERs (with a total capacity of 83 MW) could not meet the LVRT requirement and were tripped. Also, the figure points out that this net load increase leads to the overloading of two parallel lines 1-3 shown by a yellow color, as the spinning reserve generators compensate the generation shortage, and this follows the current increase in the mentioned two lines.

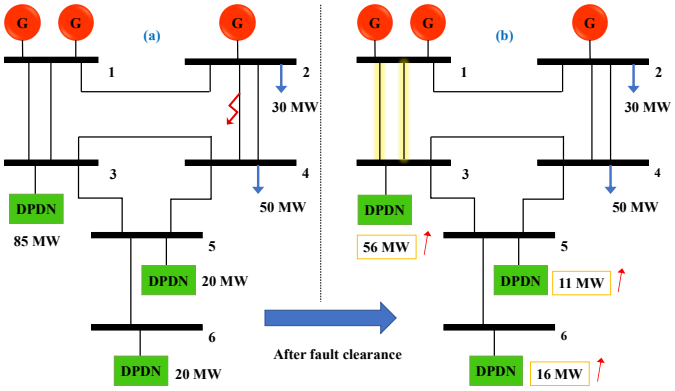

Fig. 2. Net load increase in high-voltage network by LVRT response of distribution-level DERs.

On the other hand, if this fault was single line-ground with a duration of 100 ms, the LVRT response of the DPDNs would be negligible. These are just two scenarios among a high number of scenarios with different probabilities. The critical point is that the conventional contingency analyses have been studied for failures of system components like line and generator (based on forced outage rates), majorly in N-1 and N-2 criterions as the important cases. However, this kind of source contingency analysis introduced herein concerns the net load increase in one or several buses, which may affect the system security by overloading one line or even more. Thus, about the power systems with considerable penetration of DERs, the LVRT-oriented security assessment is an essential tool for the TSO to consider the LVRT response of DPDNs and its impact on transmission system security.

The TSO can examine several faults and see their impact through the T&D simulation method, which incurs a very high computational burden. The proposed framework lets the DSOs construct the LVRT response functions and send them to the TSO. Using these functions, the TSO conducts the security assessment to obtain the overloading risk. It should be noted that these functions are almost independent of the system pre-contingency operating point. For example, a 1% demand increase in buses 2-6 (due to the temperature increase) does not imply reconstructing the response functions for each DPDN. This function-based approach gives the opportunity of conducting the security assessment in a short computation time efficiently.

As a conclusion, the main contributions of this paper are enumerated below.

1) LVRT analysis of DPDNs through a general mathematical model (the DAE system formation) is addressed to find the DERs' response to the voltage sags. DSOs use this tool to construct the LVRT response function of DPDNs.
2) Introducing the Haar wavelets and explaining the application of the Haar expansion method in approximating the LVRT response function of DPDNs.
3) Discussing the LVRT-oriented security assessment of the transmission systems from the analytical viewpoint. The TSO uses the LVRT response functions provided by DSOs to check the system security and evaluate the risk of overloading through the MCS.

After the introduction and explaining the contribution, the rest of the paper is organized as follows. Section II gives a full explanation of the problem. Section III discusses the mathematical model and problem formulation. Section IV examines the proposed model in two small and large-scale systems, and the final section provides the conclusion.

II. Problem Definition

This problem is a source contingency analysis to evaluate the loading security of transmission systems. The DERs' response (in distribution level) to the voltage sags impacts the transmission lines loading in the post-clearance condition of the system. Thus, the TSO requires a security assessment method to achieve the overloading risk with sufficient time. The first step in this approach is the LVRT analysis to get the DPDNs' LVRT response for any transient faults in the transmission system. It means that the TSO has to model the distribution sector and conduct the LVRT analysis, which is time-consuming. A function-based source contingency is proposed to eliminate this step for the TSO that dramatically lessens the simulation time. This method lets the TSO get the LVRT response of DPDNs for any random fault without LVRT analysis. Besides, the DSOs are responsible for constructing the LVRT response functions. The LVRT response function gives the lost DER capacity for the input sag depth and duration related to the DPDN's HV/MV bus. This function is achieved through the LVRT analysis of the DPDN (Section II-B) and is applicable for the TSO until the update is required. The DSO updates the function and resends it to the TSO whenever the corresponding DER capacity or network configuration changes. As it was investigated in [28], the demand variations and even load growth have not a substantial effect on the LVRT capability of the DPDNs. Nevertheless, DSOs can annually update these functions. This is an advantage for the TSO to implement these functions independently of the pre-contingency operating point of the system.

Considering the given explanation, the problem formulation is presented in three subsections. Subsection A addresses the mathematical model of the LVRT analysis, which is a tool for the DSO to construct the LVRT response function. The LVRT response function definition is discussed in subsection B. And

the LVRT-oriented security assessment model is presented in subsection C. However, three points must be mentioned before later discussions. First, momentary cessation as one of the DER responses is excluded in this study. Second, the persistent faults are ignored, and only the transient faults are considered. In this case, the switched-off faulted line is returned to the circuit after the fault clearance (this assumption is valid for most transient faults [30]). Third, the LVRT analysis is modeled through the DAE systems related to the transient undervoltage condition of the DPDN. It is assumed that the transmission sector does not experiment with the instability problems during this period. This assumption helps to model the LVRT analysis of a DPDN for voltage sags with the origin of transmission-level faults. Besides, the TSO aims to evaluate the lines' flow changes in the dynamically stable post-clearance condition of the system. Thus, the static security assessment serves the goal.

A. LVRT analysis of DPDNs

For a DPDN with different LVRT categories of DERs, LVRT analysis is a tool to get the variations in PCC voltage of DERs during the abnormal voltage condition and to determine the tripped DERs which cannot meet their LVRT requirement. This work implies appropriate dynamic modeling of DERs including synchronous fossil-fuel generators and inverter-interfaced generators. Note that based on the IEEE 1547 standard, the minimum phase voltage is taken into account to check the meeting of the LVRT requirement. It is worth mentioning that this model should consider the symmetric and asymmetric voltage sags applied to the DPDN. The general model of LVRT analysis in the dq reference frame is formulated as follows.

1) Synchronous generators: These types of generators are included in Category I DERs and have the general form of differential-algebraic equations (DAE) in (1) for kth unit [28]. These equations are valid in positive sequence and for negative and zero sequences, just their transient reactance is modelled.

$$\begin{cases} \dfrac{d\mathbf{x}_k^{sg}}{dt} = f^{sg}(\mathbf{x}_k^{sg}, \mathbf{z}_k^{sg}, \mathbf{u}_k^{sg}) \\ 0 \quad = g^{sg}(\mathbf{x}_k^{sg}, \mathbf{z}_k^{sg}, \mathbf{u}_k^{sg}) \end{cases} \tag{1}$$

In this system of DAE, $\mathbf{x}^{sg}$, $\mathbf{z}_k^{sg}$ are the differential and algebraic vector variables respectively and $\mathbf{u}^{sg}$ is the time-variant input variable vector.

2) Inverter-interfaced generators: Inverter-interfaced generators are accounted as Category II DERs and their general model for the kth unit is formulated in a DAE form like (2). This system of DAE consists of both the positive and negative sequences.

$$\begin{cases} \dfrac{d\mathbf{x}_k^{ig,\pm}}{dt} = f^{ig}(\mathbf{x}_k^{ig}, \mathbf{z}_k^{ig}, \mathbf{u}_k^{ig})^{\pm} \\ 0 \quad = g^{ig}(\mathbf{x}_k^{ig}, \mathbf{z}_k^{ig}, \mathbf{u}_k^{ig})^{\pm} \end{cases} \tag{2}$$

All the relative differential and algebraic equations can be found in [28]. However, these DERs require a proper reactive current injection strategy to better ride through the abnormal voltage condition. Equations (3)-(6) are used as the LVRT strategy to set the current references in positive and negative sequences [31].

$$V_k^m = \min\{V_k^a, V_k^b, V_k^c\} \tag{3}$$

$$Q_k^* = \begin{cases} 0, & V_k^m \geq 0.9 \\ 1.428(0.9 - V_k^m)S_k^*, & 0.2 \leq V_k^m < 0.9 \\ S_k^*, & V_k^m < 0.2 \end{cases} \tag{4}$$

$$P_k^* = \sqrt{(S_k^*)^2 - (Q_k^*)^2} \tag{5}$$

$$\begin{bmatrix} i_d^{*,+} \\ i_q^{*,+} \\ i_d^{*,-} \\ i_q^{*,-} \end{bmatrix} = \begin{bmatrix} v_d^+ \\ v_q^+ \\ -v_d^- \\ -v_q^- \end{bmatrix} \frac{P^*}{v_\alpha - v_\beta} + \begin{bmatrix} v_q^+ \\ -v_d^+ \\ v_q^- \\ -v_d^- \end{bmatrix} \frac{Q^*}{v_\alpha + v_\beta} \tag{6}$$

Here v^m is the minimum phase voltage in time t, $v_\alpha = (v_d^+)^2 + (v_q^+)^2$ and $v_\beta = (v_d^-)^2 + (v_q^-)^2$.

3) Network equations: Network algebraic equations considering positive and negative sequences in the DQ reference frame are as (7). G and B matrices are extracted from the reduced form of the admittance matrix.

$$\begin{bmatrix} G & -B \\ B & G \end{bmatrix}^{\pm} \begin{bmatrix} V_D \\ V_Q \end{bmatrix}^{\pm} = \begin{bmatrix} I_D \\ I_Q \end{bmatrix}^{\pm} \tag{7}$$

The variable vectors $V_{DQ}^{\pm}$ and $I_{DQ}^{\pm}$ respectively denote the bus voltages and bus injection currents. The first element of these vectors relates to the HV/MV substation bus and its injection current is calculated by sag depth and the fault type in transmission sector. These equations must be reformulated in the dq reference frame through (8) and (9) to shift the individual dq reference frames to the common reference frame DQ.

$$T = \begin{pmatrix} \cos\delta & \sin\delta \\ -\sin\delta & \cos\delta \end{pmatrix} \tag{8}$$

$$T^{-1} \begin{bmatrix} G & -B \\ B & G \end{bmatrix}^{\pm} T \begin{bmatrix} V_D \\ V_Q \end{bmatrix}^{\pm} = \begin{bmatrix} I_D \\ I_Q \end{bmatrix}^{\pm} \tag{9}$$

Considering the above-mentioned differential and algebraic equations, the overall system of DAE can be solved by the trapezoidal method and through the algorithm explained in [28]. The ultimate matrix equality is given in (10), in which $\mathbf{\Lambda}_t$ is the time-variant matrix of coefficients and $\mathbf{U}_t$ is the time-variant output vector.

$$\mathbf{\Lambda}_t^{\pm} \begin{bmatrix} \mathbf{x} \\ \mathbf{z} \end{bmatrix}^{\pm} = \mathbf{U}_t^{\pm} \tag{10}$$

Note that in each time step the LVRT condition of each DER is checked. If the LVRT requirement of any DER is not met, the DER is tripped and its relevant differential and algebraic equations are omitted. This omission results in the updated form of these three matrices. Using this model, the LVRT behavior of the DERs and the lost capacity at the end of sag duration are obtained.

B. Haar wavelets

The previous subsection represented a general mathematical model to get the lost DER capacity of a DPDN in response to a voltage sag on the HV/MV substation. There are several methods of numerical function approximation like the Fourier approach that uses the available sample points to have a Fourier-based function. Nevertheless, LVRT response of DPDNs takes specific and discrete values (total capacity of tripped DERs) for the applied voltage sags. Also, the sag depth on the HV/MV substations ζ and the sag duration τ are the required function inputs to calculate the LVRT response of DPDNs. Since a function with continuous inputs and discrete output is required, this paper proposes the 2D Haar expansion to approximate the LVRT response function of DPDNs [32]. Haar expansion implemented here is composed of Haar scaling functions as the father wavelet (11) and can fulfil the mentioned requirement with existing sample points. However, the standard form of the scaling function is as (12), in which m is the resolution index and n is the translation coefficient [33].

$$\varphi(x) = \begin{cases} 1, & 0 \le x \le 1 \\ 0, & \text{otherwise} \end{cases} \tag{11}$$

$$\varphi_{m,n}(x) = 2^{m/2}\varphi(2^m x - n) \tag{12}$$

Ref. [34] explained the voltage sag characteristic and modelled the phase voltages of HV/MV substations using the sag depth for different types of faults in the transmission sector. This enables us to produce these sample points through LVRT analysis. Indeed, the DSO implements the LVRT analysis to find the lost DER capacity for each defined voltage sag. Thus, for $2^m \times 2^{m'}$ sample points, the LVRT response function H is approximated through 2D Haar series with m, m' indices of resolution and for fault type j as follows.

$$H_{m,m',j}(\tau,\zeta) = \sum_{n=0}^{2^m-1}\sum_{n'=0}^{2^{m'}-1} K_{n,n',j}.\phi_{n,m,n',m'}(\tau,\zeta) \tag{13}$$

$$\phi_{n,m,n',m'}(\tau,\zeta) =$$

$$\varphi(2^m(\tau-\underline{\tau}) - n\Delta_\tau)\varphi(2^{m'}(\zeta-\underline{\zeta}) - n'\Delta_\zeta) \tag{14}$$

$$\Delta_\tau = \bar{\tau} - \underline{\tau},\ \ \Delta_\zeta = \bar{\zeta} - \underline{\zeta} \tag{15}$$

Here 4 types of 1) single-phase-ground (SLG), 2) line-line (LL), 3) line-line-ground (LLG) and 4) 3PH are considered respectively. $K_{n,m,j}$ as the Haar series coefficient stands for the lost DER capacity in nth sag duration and n'th sag depth for the jth fault type. Δ is the difference symbol.

Look at Fig. 3 with 9×7 sample points identified by sag duration and sag depth on the HV/MV substation. The sample points denote the LVRT response output of a DPDN extracted by the LVRT analysis in 7 sag depth and 9 sag duration values. These sample points create the 2D LVRT response function, in which each square belongs to a Haar coefficient value represented by specific color. Therefore, the DSO uses a limited number of sample points to construct the LVRT response function that is valid for any input values of sag depth and duration.

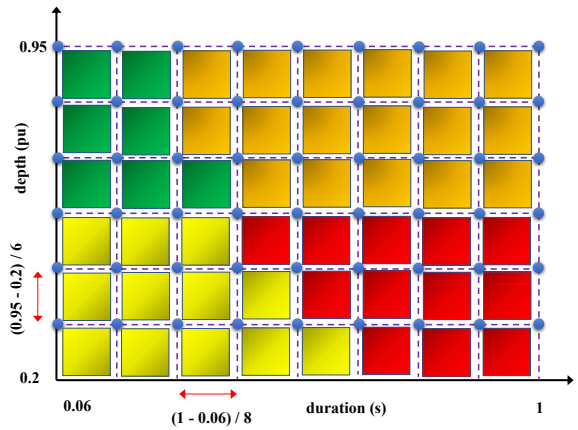

Fig. 3. Constructing LVRT response function using sample points of sag depth and duration.

C. LVRT-oriented security assessment

After approximating the LVRT response functions for all the DPDNs, it is the turn of LVRT-oriented security assessment in the transmission sector. The TSO uses the available LVRT response functions to conduct the static security assessment within the source contingency framework. This security assessment implements the MCS method to get the overloading risk of transmission lines. The flowchart in Fig. 4 provides a general outline of the whole process to assess the transmission system security through the MCS. First, MCS requires the probability distribution of fault type, faulted line, fault location, and fault clearing time [30].

1) Fault type: With consideration of $\mathbf{p}^{ft} = \{69.8\%, 5\%, 10.6\%, 14.6\%\}$, the related multinomial probability distribution as a function of the decision vector, $\mathbf{w}$ is

$$F^{ft}(\mathbf{w}|\mathbf{p}) = \prod_{j\in\Omega_T} (p_j^{ft})^{w_j} \tag{16}$$

2) Faulted line: The probability distribution related to fault occurrence in transmission lines can be obtained by (17) and (18).

$$p_\ell^{fl} = \frac{\lambda_\ell}{\sum_{\ell\in\Omega_L}\lambda_\ell} \tag{17}$$

$$F^{fl}(\mathbf{w}|\mathbf{p}) = \prod_{\ell\in\Omega_L} (p_\ell^{fl})^{w_\ell} \tag{18}$$

3) Fault location: Fault location in a line has a uniform probability distribution and can be determined in the MCS process by generating a random number between [0-1].

4) Fault clearing time: However, fault clearing time follows a normal probability distribution, but it depends on three conditions of relay operation: primary, secondary, and tertiary protection. The respective expected values (μ) and standard deviations (σ) of the probability distribution F^{fc} are $\{69.8\%, 5\%, 10.6\%, 14.6\%\}$.

$$F^{fc}(\tau|\mu,\sigma) = \frac{1}{(2\pi\sigma^2)^{1/2}} \exp\{\frac{(\tau-\mu)^2}{2\sigma^2}\} \tag{19}$$

In each iteration of the MCS e, random values of these fault parameters are extracted by (20). Then, the sag depths

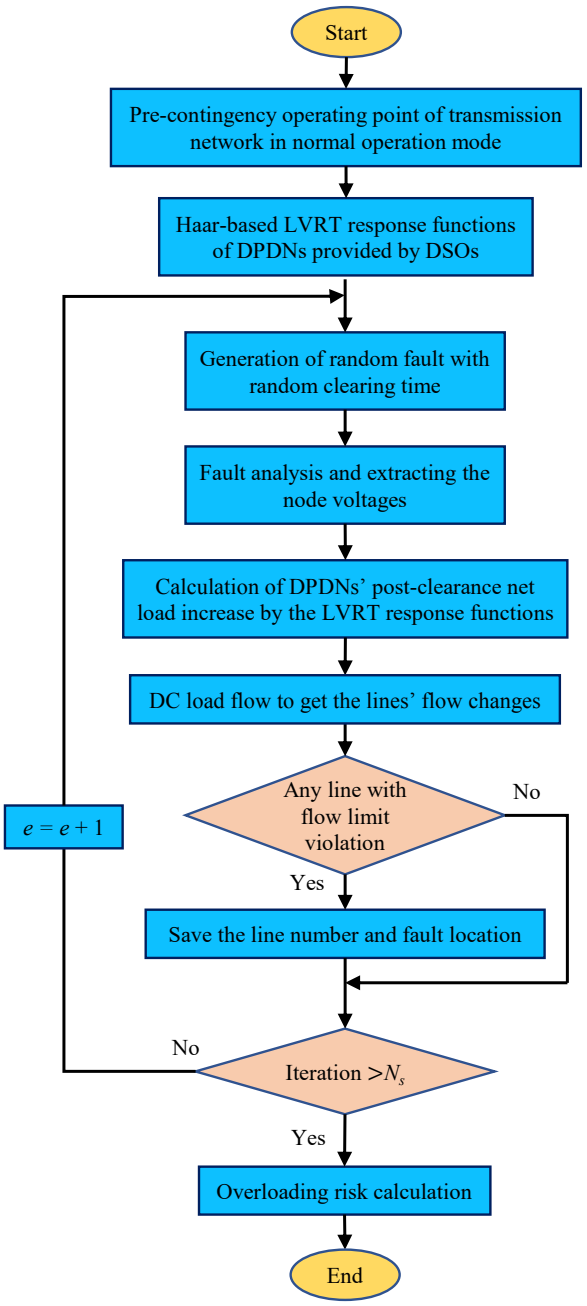

Fig. 4. Flowchart of the process for LVRT-oriented security assessment.

of transmission buses are calculated in each iteration through the fault analysis as (21). So, the sag duration and sag depth as the two inputs of the individual LVRT response function of the DPDNs are obtained in each iteration.

$$FT^e = \Re\{F^{ft}\},\ FL^e = \Re\{F^{fl}\},\ \tau^e = \Re\{F^{fc}\}, \tag{20}$$

$$\zeta^e = \Im\{FT^e, FL^e\} \tag{21}$$

Now to assess the overcurrent risk of the transmission lines (in the post-clearance dynamically stable condition); first, the pre-contingency operating point of the transmission network is required. This is achieved through the well-known power flow equations as below, where $|.|$ and $\angle$ denote the admittance absolute and angle, respectively.

$$P_i^g - P_i^d = \sum_{i' \in \Omega_B} |Y_{i,i'}||V_i||V_{i'}| \cos(\theta_{i'} - \theta_i + \angle Y_{i,i'}) \tag{22}$$

$$Q_i^g - Q_i^d = -\sum_{i' \in \Omega_B} |Y_{i,i'}||V_i||V_{i'}| \sin(\theta_{i'} - \theta_i + \angle Y_{i,i'}) \tag{23}$$

Then using the constructed LVRT response functions, one can obtain the flow changes of lines in each MCS scenario through (24)-(27).

$$P_i^{sr} - \gamma_i H_i(\tau, \zeta_i) = \sum_{i' \in \Omega_B} B_{i,i'}(\Delta\theta_i - \Delta\theta_{i'})S_b \tag{24}$$

$$\forall A(i,\ell) = A(i^{'},\ell) = 1$$

$$\Delta J_\ell = B_{i,i'}(\Delta\theta_i - \Delta\theta_{i'})S_b \tag{25}$$

$$E_\ell = \begin{cases} 1, & J_\ell^{pc} + \Delta J_\ell \geq \bar{J}_\ell \\ 0, & J_\ell^{pc} + \Delta J_\ell < \bar{J}_\ell \end{cases} \tag{26}$$

$$\chi = \begin{cases} 1, & \sum_{\ell \in \Omega_L} E_\ell \geq 1 \\ 0, & \sum_{\ell \in \Omega_L} E_\ell = 0 \end{cases} \tag{27}$$

Equation (24) stands for the DC power flow to compute the change in node angles. Binary parameter γ is 1 if a DPDN is connected to bus i. In (25), matrix A is the incidence matrix showing the connection state of line ℓ to bus i and ΔJ denotes the flow changes in lines relative to the pre-contingency amount. The loading limit violations for each transmission line and the whole system are respectively determined in (26) and (27), by variables E_ℓ and χ. In the end, the risk of line overloading is calculated for a transmission system in N_s iterations as (28). This risk index captures the probability that the system is exposed to line overloading. As the risk index increases, the expected LVRT-oriented security margin of the transmission network decreases. This means that the system is vulnerable to line overloading and subsequent difficulties (like cascading outages) in higher risk values.

$$\Gamma = \frac{1}{N_s}\sum_{e=1}^{N_s} \chi^e \tag{28}$$

III. Results and Discussions

In this section, the proposed approach is verified and evaluated in two case studies of the Roy Billinton Test System (RBTS) and New England IEEE 39 bus system. RBTS is a small-scale test system that can be applicable in this paper since both of its transmission and distribution level structures are available for the researchers, and the 39 bus system with a larger scale can enhance validity of the results. Also, in this section first, the results about the LVRT analysis of the introduced DPDNs are evaluated. Then, the LVRT response functions of the DPDNs and the security assessments in the test systems are discussed. All the simulations are carried out in MATLAB script environment in a Core i5 Laptop with 4GB RAM.

TABLE I
REQUIRED DATA FOR DERS WITHIN THE DPDNS

Bus	DER capacity (MW)	DER location	DER category
3	1,5,1.5,4,2,2,2	3,11,17,27,37,42,44	II,II,I,II,I,II,II
	2.5,1,5,4,5,10	53,58,61,67,70,76	I,I,II,II,I,I
5	2,0.8,0.5,3	11,19,31,37	II,II,II,I
6	1,3,1,2,1,4	12,24,34,41,53,58	I,II,II,I,II,II

A. Test network

The RBTS is a 230 kV 6-bus power system [35] that its modified network is shown in Fig. 5. This modified network consists of three DPDNs, two conventional load buses, and three thermal plants with capacities of 100, 110, and 130 MW. It is assumed that the spinning reserve capacities of 60 MW and 40 MW are available in bus 1. The pre-fault loads of the DPDNs buses seen from the transmission sector are given in the figure, and the scheduled powers of the thermal units are 20.85 MW, 60 MW, and 119.47 MW, respectively. The

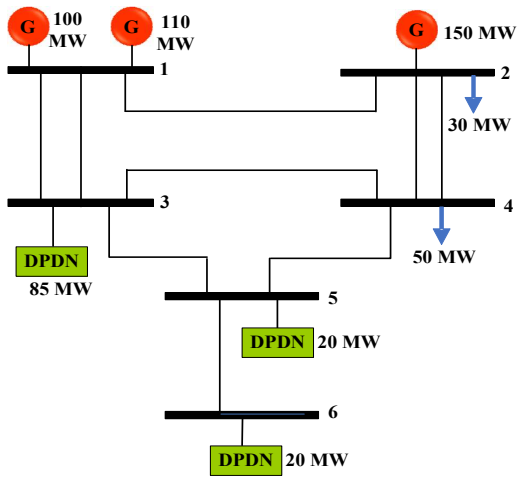

Fig. 5. Schematic of modified 6 bus RBTS.

bus data and line data of the distribution networks (buses 3, 5, 6 of the RBTS) can be found in [36]. Also, their pure load is increased so that the DER penetration level lies between 40-50% for each network. However, Table I gives the required data about the capacities, locations, and LVRT categories of the DER installed in each feeder of these three networks. It is noteworthy that Bus numbers in these three distribution networks are 1 point greater than the shown line numbers in [36]. Also, it should be noted that the whole LV side of the distribution network is not taken into account for LVRT analysis. However, any LV network with considerable PV capacity is modeled for the MV side analysis through an assumed Thevenin impedance and aggregated PV capacity (connected to MV bus). To achieve this equivalent model of LV distribution networks, several methods have been introduced. The proposed method in [37] is implemented in this paper, which assumes a uniform load and PV capacity distribution on all its nodes.

B. LVRT behavior of the DPDNs

First of all, to verify the validity of the mentioned model for LVRT analysis of the DPDNs, the LVRT capability of DERs concerning different voltage sags is evaluated. Note that regions 4 and 5 of the LVRT capability curves for both the categories are assumed to be ride-through and shall-trip respectively, which is a pessimistic criterion. Also, it is worth mentioning that the feeders and loads are not pure resistive and are assumed to have an additional inductive consumption. Fig. 6 represents the LVRT behavior of the 6 DERs (three of them are aggregated models) for sag depth of 50% on the 33/11 kV substation and sag duration of 340 ms, for fault type 1. It represents the per unit (pu) PCC voltage variations for the DERs of the DPDN connected to bus 6 of the RBTS. Since the least voltage among the three phases is the base, the DERs are all tripped due to incapability in meeting their LVRT requirement. The first DER with Category I performance is tripped after 160 ms and the remaining ones are tripped over 320 ms.

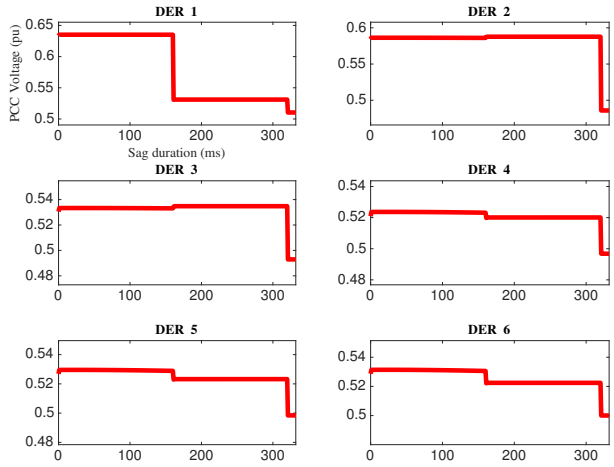

Fig. 6. Phase A voltage of the DERs in 33/11 kV substation of RBTS6 for $FT = 1, \zeta = 50\%, \tau = 340$.

Fig. 7 shows the voltage variation of the DERs in bus 3 of the RBTS, first substation including feeders 1 and 2, and for the same above-mentioned sag condition. It can be seen that despite the reactive power injection by the DERs and increasing the PCC voltages, they cannot meet the LVRT requirement for this sag duration. If the sag duration was less than 320 ms, Category II DERs were able to stay connected. The behavior of these DERs for 3PH fault is represented in Fig. 8, where the PCC voltages are close to 0.5 pu due to the severity of the sag.

Now if the sag depth increases to 80% for fault type of 3, it can be seen in Fig. 9 that the voltage of phase B has an acceptable increase up to 320 ms. This refers to the reactive power injection strategy that directly depends on the PCC voltage and injects more reactive power in a higher depth of the voltage sag.

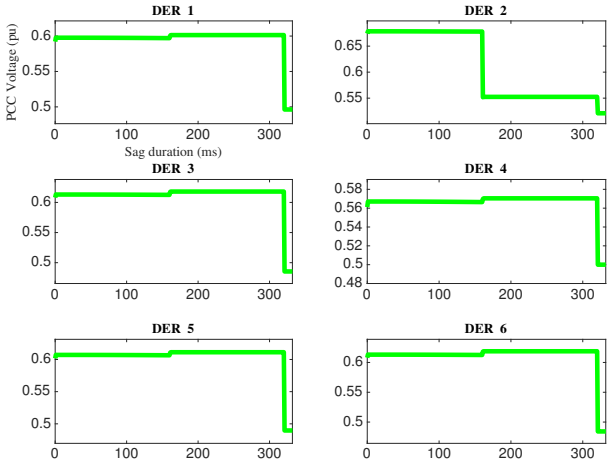

Fig. 7. Phase A voltage of the DERs in 33/11 kV substation of RBTS3 for $FT = 1, \zeta = 50\%, \tau = 340$.

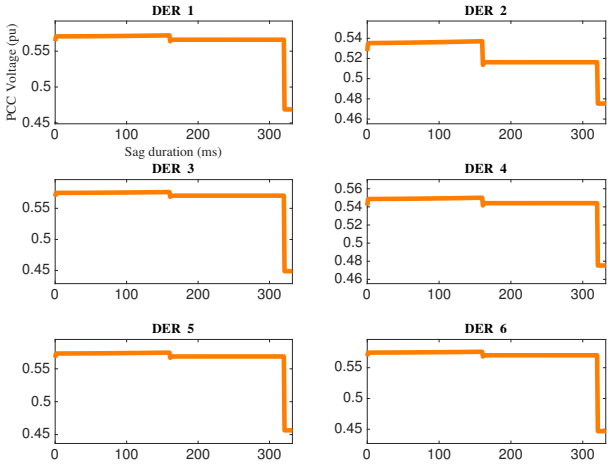

Fig. 8. Phase A voltage of the DERs in 33/11 kV substation of RBTS3 for $FT = 4, \zeta = 50\%, \tau = 340$.

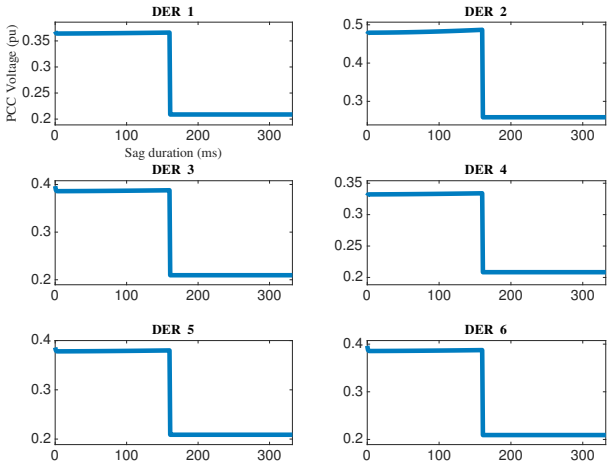

Fig. 9. Phase B voltage of the DERs in 33/11 kV substation of RBTS3 for $FT = 3, \zeta = 80\%, \tau = 340$.

C. LVRT-oriented security assessment of the RBTS

The LVRT-oriented security assessment of the 6-bus RBTS transmission system requires the LVRT response functions for each 3 DPDNs. These functions are constructed by the DSOs of the DPDNs and are provided for the TSO to conduct the overloading security assessment. The corresponding 2D Haar series coefficients of the DPDNs connected to buses 3, 5, and 6 are depicted for different fault types in Figs 10-12. These figures map the matrix of lost DER capacity (obtained by sample values of sag depth and duration) to different colors. The blue regions stand for the lower loss of DERs and more successful ride-through; however, the red regions denote the higher lost capacity. By looking at these three figures, the DPDNs exhibit the highest LVRT capability in faults of type 1. Its reason is that the blue regions, which denote the more un-tripped DER capacity, are dominant in sag durations of less than 400 ms. This region includes the protection clearing times of zones 1 and 2, which are more probable than the third protection zone. It is seen in Fig. 10 (fault types 3 and 4) that the sag depth values above 0.6 pu for the duration of about 200-350 ms and also the depth values above 0.4 pu for durations of greater than 350 ms encounters the DPDN to lose all its generation capacity. For fault type 2, these values increase to about 0.8 and 0.55 pu, respectively. This is almost the same for the other DPDNs. The mentioned intervals of sag depth and duration belong to the protection zones 2 and 3 that may have low probability but can significantly impact the bulk system security.

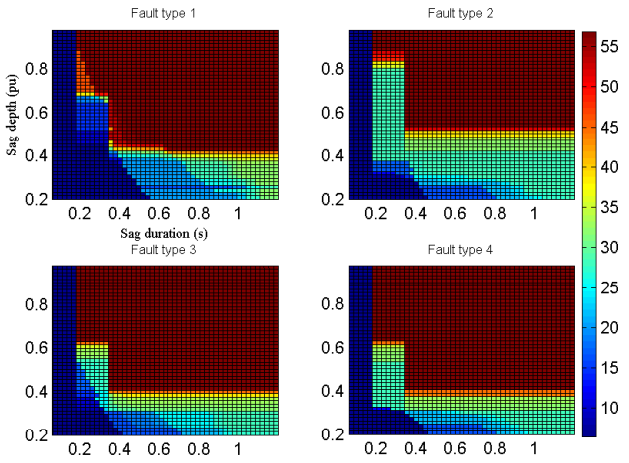

Fig. 10. Haar series coefficients of Bus 3 DPDN for each fault type.

Using these represented coefficients, the LVRT response function of each DPDN is approximated through the 2D Haar series. These functions let the TSO implement the source contingency and get the (post-clearance) net load increase of each DPDN for any fault. By running the MCS with an iteration number of 2000 (applying 2000 random faults), the LVRT-oriented security of the transmission system is evaluated in 2 s. The derived outcome shows that the two parallel lines between buses 1 and 3 may face the overcurrent danger, both with the probability of 30%. In other words, a transient fault can expose the existing secure transmission system to line overloading with a 30% probability. Therefore, there is

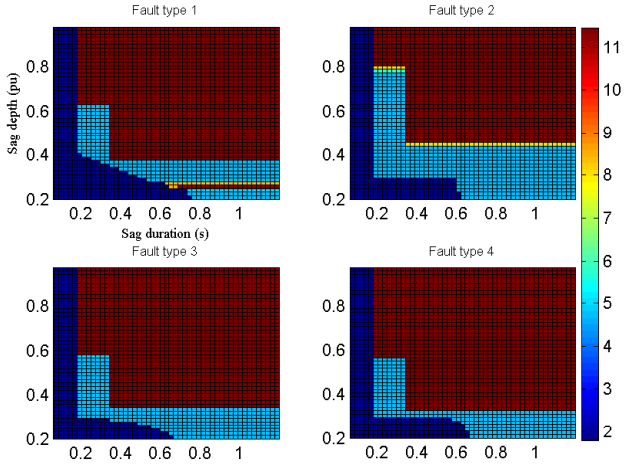

Fig. 11. Haar series coefficients of Bus 5 DPDN for each fault type.

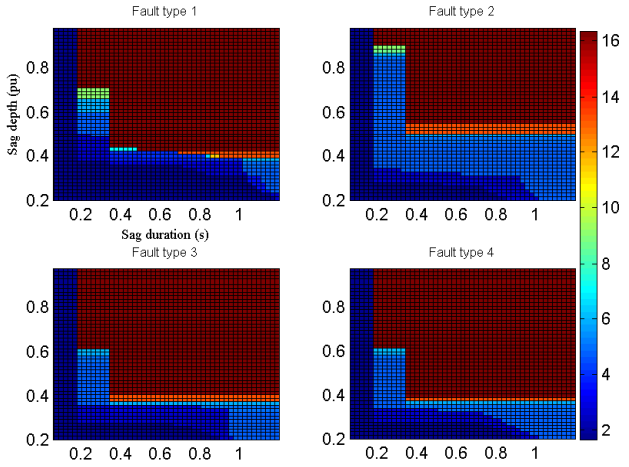

Fig. 12. Haar series coefficients of Bus 6 DPDN for each fault type.

a probability of 70% for the LVRT-based secure operation of the RBTS transmission system.

D. DERs' response to voltage sags with optimistic criterion

The LVRT analysis of the DPDNs and the security assessment of the transmission system were carried out in previous subsections based on the DERs' response to voltage sags with a pessimistic criterion. On this base, the fifth zone of the LVRT capability curves was considered as the shall-trip zone by the TSO and this refers to the inference about the DERs and their reliability issues under voltage sags. However, if the TSO considers this zone as the ride-through performance for the two regarded LVRT categories, the DERs within the DPDNs will have different LVRT behavior during the voltage sags. Note that the DSOs construct the LVRT response functions with respect to the performance standard determined by the TSO. With this optimistic criterion, the Haar series coefficients of the LVRT response function for the bus 3 DPDN is shown in Fig. 13.

As it is seen, the regions with low DER lost capacity are dominant in these LVRT response function coefficients. This refers to enhancing the ride-through ability of the DERs and

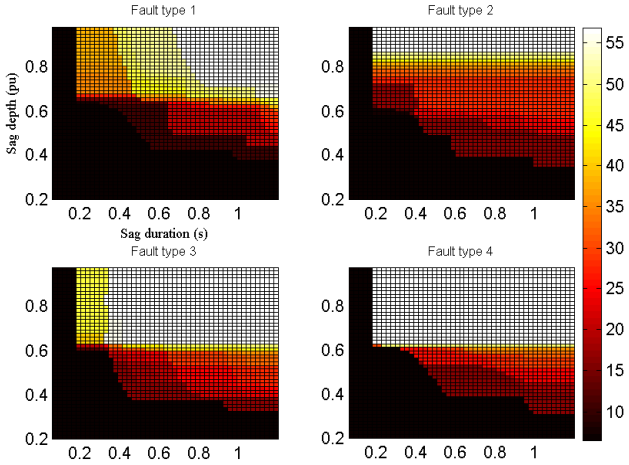

Fig. 13. Haar series coefficients of Bus 3 DPDN for optimistic-based LVRT curve.

lowering the trip zone in the LVRT capability curves for different performance categories. Consider the two fault types of LL and 3PH. Comparing with the Haar series coefficients obtained in Fig. 10, it is observed that the worst cases (trip of all DERs) in the pessimistic criterion and for these fault types almost occur at sag depths of higher than 57% and 40% respectively. While by adopting the optimistic criterion, the least sag depth values that cause the trip of all the DERs within the DPDN are about 83% and 60% respectively for LL and 3PH fault types. Although this shows a substantial enhancement in the LVRT capability of the DPDN, it should be noted that the tolerance of DERs against the voltage sags highly affects the operator strategy in determining the DER response curve. Besides, in this case, the LVRT-oriented security assessment gives the overcurrent risk value of 8% in the same lines mentioned above, which represents a substantial reduction compared to the previous case and an increase in the security margin of the system.

E. IEEE 39 bus system

In this case study, the proposed concept is examined in the New England IEEE 39 bus system shown in Fig. 14 as a more extensive network. The network has ten generators that those connected to buses {32-35,37} are supposed to be the spinning reserve generators. Also, the green rectangles are the original aggregated loads replaced by the rescaled DPDNs aforementioned in the previous case study and are specified by RBTS buses numbers. Furthermore, the loading of all lines is 1 kA except the line between 21-22 that is increased to 1.1 kA.

The associated results are obtained through 5000 scenarios and with the elapsed running time of 1.64 min. Considering the pessimistic-based LVRT capability curves and after conducting the LVRT-oriented security assessment, the system is exposed to the overloading problem with the probability of about 25% as the risk of security violation. The lines 5-6 and 16-19 are subjected to the risk of overcurrent with probabilities of 24% and 16% respectively. Furthermore, Table II gives the line numbers exposed to the loading of over 80% with their

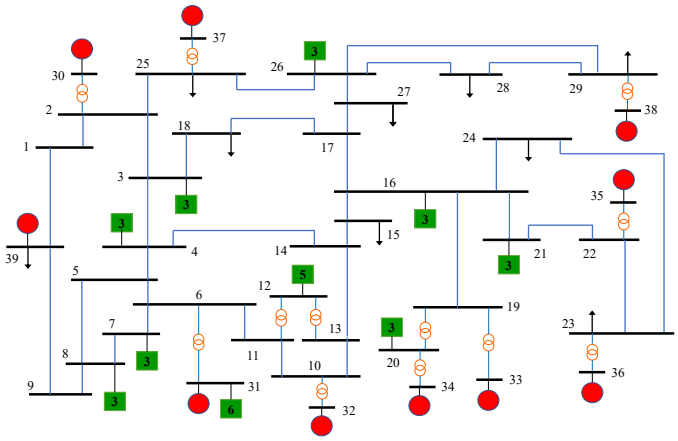

Fig. 14. Schematic of IEEE 39 bus test system.

TABLE II
LINES WITH PROBABILITY OF OVER 80% LOADING

Line (bus-bus)	Probability (%)	Line (bus-bus)	Probability (%)
5 - 6	24	10 - 11	13
6 - 7	36	16 - 19	25
6 - 11	04	21 - 22	48

related probability, which states that these lines are in danger of the alarm condition. It is noteworthy that in this network, the adoption of optimistic criteria results in a negligible risk of overloading. However, this cannot be taken as a rule, and the power systems with higher penetration levels are more exposed to security violations.

IV. Conclusion

This work studied the negative impact of the DPDNs' LVRT response on transmission system security. DERs' response to abnormal voltages and their failure to meet the LVRT requirement can impose a significant risk to the bulk power system. This risk stems from the trip of the DERs in the distribution level and consequently the net load increase in the transmission sector. The trip of DERs resulting from transmission-level faults is the so-called source contingency. This kind of contingency analysis concerns the impact of lost distribution-level generation on the transmission line loading. It was observed that the DPDNs have different behaviors against the various voltage sags. The DPDNs with a high percentage of Category I DERs have weak LVRT capability and are more vulnerable to lose a considerable part of their capacity over the sag duration. As it was completely explained, involving the LVRT analysis of each DPDN in the security assessment process dramatically increases the simulation time. To overcome this obstacle, a 2D Haar-based function was defined for each DPDN to model their lost capacity over the sag duration, which simplified the LVRT-oriented security assessment of the system. These functions are constructed by the DSOs and are provided for the TSO to conduct the source contingency irrespective of distribution-level model and LVRT analysis. As mid-term load growths (for 5-8 years) roughly affect the LVRT response functions, the TSO can implement them independently of the system operating point. However, the function requires the update whenever the DER capacity or network configuration of the DPDN is changed.

References

[1] Y. Han, Y. Feng, P. Yang, L. Xu, Y. Xu, and F. Blaabjerg, "Cause, classification of voltage sag, and voltage sag emulators and applications: a comprehensive overview," *IEEE Access*, vol. 8, pp. 1922–1934, 2019.

[2] D. G. Photovoltaics and E. Storage, "IEEE standard for interconnection and interoperability of distributed energy resources with associated electric power systems interfaces," *IEEE Std*, pp. 1547–2018, 2018.

[3] A. Mojallal and S. Lotfifard, "Enhancement of grid connected PV arrays fault ride through and post fault recovery performance," *IEEE Transactions on Smart Grid*, vol. 10, no. 1, pp. 546–555, 2017.

[4] Y. Geng, K. Yang, Z. Lai, P. Zheng, H. Liu, and R. Deng, "A novel low voltage ride through control method for current source grid-connected photovoltaic inverters," *IEEE Access*, vol. 7, pp. 51 735–51 748, 2019.

[5] C. Kim and W. Kim, "Enhanced low-voltage ride-through coordinated control for PMSG wind turbines and energy storage systems considering pitch and inertia response," *IEEE Access*, vol. 8, pp. 212 557–212 567, 2020.

[6] H. Dong, N. Chen, X. Li, and H. Li, "Improved adaptive robust control for low voltage ride-through of front-end speed regulation wind turbine," *IEEE Access*, vol. 8, pp. 55 438–55 446, 2020.

[7] O. P. Mahela, N. Gupta, M. Khosravy, and N. Patel, "Comprehensive overview of low voltage ride through methods of grid integrated wind generator," *IEEE Access*, vol. 7, pp. 99 299–99 326, 2019.

[8] C. Kim and W. Kim, "Coordinated fuzzy-based low-voltage ride-through control for pmsg wind turbines and energy storage systems," *IEEE Access*, vol. 8, pp. 105 874–105 885, 2020.

[9] L. Ji, J. Shi, Q. Hong, Y. Fu, X. Chang, Z. Cao, Y. Mi, Z. Li, and C. Booth, "A multi-objective control strategy for three phase grid-connected inverter during unbalanced voltage sag," *IEEE Transactions on Power Delivery*, 2020.

[10] G. Sun, Y. Li, W. Jin, S. Li, and Y. Gao, "A novel low voltage ride-through technique of three-phase grid-connected inverters based on a nonlinear phase-locked loop," *IEEE Access*, vol. 7, pp. 66 609–66 622, 2019.

[11] G. Lammert, D. Premm, L. D. P. Ospina, J. C. Boemer, M. Braun, and T. Van Cutsem, "Control of photovoltaic systems for enhanced short-term voltage stability and recovery," *IEEE Transactions on Energy Conversion*, vol. 34, no. 1, pp. 243–254, 2018.

[12] M. Choopani, S. H. Hosseinian, and B. Vahidi, "New transient stability and LVRT improvement of multi-VSG grids using the frequency of the center of inertia," *IEEE Transactions on Power Systems*, vol. 35, no. 1, pp. 527–538, 2019.

[13] C. Mishra, A. Pal, J. S. Thorp, and V. A. Centeno, "Transient stability assessment of prone-to-trip renewable generation rich power systems using lyapunov's direct method," *IEEE Transactions on Sustainable Energy*, vol. 10, no. 3, pp. 1523–1533, 2019.

[14] W. Qian, N. Zhou, J. Wu, Y. Li, Q. Wang, and P. Guo, "Probabilistic short-circuit current in active distribution networks considering low voltage ride-through of photovoltaic generation," *IEEE Access*, vol. 7, pp. 140 071–140 083, 2019.

[15] H.-J. Lee, S.-H. Lim, and J.-C. Kim, "Application of a superconducting fault current limiter to enhance the low-voltage ride-through capability of wind turbine generators," *Energies*, vol. 12, no. 8, p. 1478, 2019.

[16] C. Huang, Z. Zheng, X. Xiao, and X. Chen, "Enhancing low-voltage ride-through capability of PMSG based on cost-effective fault current limiter and modified WTG control," *Electric Power Systems Research*, vol. 185, p. 106358, 2020.

[17] L. Djilali, E. N. Sanchez, F. Ornelas-Tellez, A. Avalos, and M. Belkheiri, "Improving microgrid low-voltage ride-through capacity using neural control," *IEEE Systems Journal*, vol. 14, no. 2, pp. 2825–2836, 2019.

[18] W.-G. Lee, T.-T. Nguyen, H.-J. Yoo, and H.-M. Kim, "Low-voltage ride-through operation of grid-connected microgrid using consensus-based distributed control," *Energies*, vol. 11, no. 11, p. 2867, 2018.

[19] I. Sadeghkhani, M. E. H. Golshan, A. Mehrizi-Sani, and J. M. Guerrero, "Low-voltage ride-through of a droop-based three-phase four-wire grid-connected microgrid," *IET Generation, Transmission & Distribution*, vol. 12, no. 8, pp. 1906–1914, 2018.

[20] S. Rajamand, A. Ketabi, and A. Zahedi, "A new LVRT strategy for DGs with different droop gains in islanded microgrid with various loads," *EPE Journal*, vol. 28, no. 3, pp. 116–127, 2018.

[21] M. M. Shabestary and Y. A.-R. I. Mohamed, "Autonomous coordinated control scheme for cooperative asymmetric low-voltage ride-through and grid support in active distribution networks with multiple DG units," *IEEE Transactions on Smart Grid*, vol. 11, no. 3, pp. 2125–2139, 2019.
[22] S. Mortazavian and Y. A.-R. I. Mohamed, "Dynamic analysis and improved LVRT performance of multiple DG units equipped with grid-support functions under unbalanced faults and weak grid conditions," *IEEE Transactions on Power Electronics*, vol. 33, no. 10, pp. 9017–9032, 2017.
[23] M. F. M. Arani and Y. A.-R. I. Mohamed, "Analysis and enhancement of the artificial bus method for successful low-voltage ride-through and resynchronization," *IEEE Transactions on Power Systems*, vol. 34, no. 3, pp. 1729–1739, 2018.
[24] I. I. Perpinias, N. P. Papanikolaou, and E. C. Tatakis, "Optimum design of low-voltage distributed photovoltaic systems oriented to enhanced fault ride through capability," *IET Generation, Transmission & Distribution*, vol. 9, no. 10, pp. 903–910, 2015.
[25] M. Islam, N. Mithulananthan, and M. Hossain, "Dynamic voltage support by TL-PV systems to mitigate short-term voltage instability in residential DN," *IEEE Transactions on Power Systems*, vol. 33, no. 4, pp. 4360–4370, 2017.
[26] W. Wang, "Fault induced delayed voltage recovery (FIDVR): Field validated time series power flow model and mitigation using smart inverters," Ph.D. dissertation, New York University Tandon School of Engineering, 2019.
[27] K. Skaloumpakas, J. Boemer, E. Van Ruitenbeek, M. Gibescu, and M. van der Meijden, "Response of low voltage networks with high penetration of photovoltaic systems to transmission network faults," 2014.
[28] P. Salyani, K. Zare, M. Abapour, A. Safari, and M. Shafie-Khah, "A general mathematical model for LVRT capability assessment of DER-penetrated distribution networks," *IEEE Access*, vol. 8, pp. 125 521–125 533, 2020.
[29] M. Henderson, "Impacts of transmission system contingencies on distributed generation-overview," in *ISO New-England DG forecast group meeting*, 2013.
[30] S. Faried, R. Billinton, and S. Aboreshaid, "Probabilistic evaluation of transient stability of a power system incorporating wind farms," *IET Renewable Power Generation*, vol. 4, no. 4, pp. 299–307, 2010.
[31] G. B. Huka, W. Li, P. Chao, and S. Peng, "A comprehensive LVRT strategy of two-stage photovoltaic systems under balanced and unbalanced faults," *International Journal of Electrical Power & Energy Systems*, vol. 103, pp. 288–301, 2018.
[32] S. G. Mallat, "A theory for multiresolution signal decomposition: the wavelet representation," *IEEE transactions on pattern analysis and machine intelligence*, vol. 11, no. 7, pp. 674–693, 1989.
[33] S. Lal, K. K. Shukla, and S. Keshri, "Haar wavelet expansions of signals and their applications in image processing," *International Journal of Computer Applications*, vol. 173, no. 9, pp. 1–23, Sep 2017. [Online]. Available: http://www.ijcaonline.org/archives/volume173/number9/28360-2017915317
[34] R. Zeng, H. Nian, and P. Zhou, "A three-phase programmable voltage sag generator for low voltage ride-through capability test of wind turbines," in *2010 IEEE Energy Conversion Congress and Exposition*. IEEE, 2010, pp. 305–311.
[35] R. Billinton, S. Kumar, N. Chowdhury, K. Chu, K. Debnath, L. Goel, E. Khan, P. Kos, G. Nourbakhsh, and J. Oteng-Adjei, "A reliability test system for educational purposes-basic data," *IEEE Transactions on Power Systems*, vol. 4, no. 3, pp. 1238–1244, 1989.
[36] R. Billinton and S. Jonnavithula, "A test system for teaching overall power system reliability assessment," *IEEE transactions on Power Systems*, vol. 11, no. 4, pp. 1670–1676, 1996.
[37] D. Santos-Martin and S. Lemon, "Simplified modeling of low voltage distribution networks for PV voltage impact studies," *IEEE Transactions on Smart Grid*, vol. 7, no. 4, pp. 1924–1931, 2015.